Latin American Journal of Solids and Structures
www.lajss.org

Strengthening of structurally damaged wide shallow RC beams using externally bonded CFRP plates

Abstract

Reinforced concrete wide shallow beams (WSBs) are commonly used in the joist flooring systems. The structural behavior of WSBs strengthened with carbon fiber reinforced polymer (CFRP) reinforcement was studied on isolated beams and as part of full-scale building. The effect of structural damage on the performance of WSBs flexurally strengthened with CFRP plates was investigated and presented in this paper. Eight full-scale WSBs were tested under four-point bending up to failure. Seven beams were strengthened with CFRP plates bonded to the soffit of the beams and one beam was unstrengthened serving as control. Prior to strengthening, the beams were subjected to different levels of damaging by preloading to 30-95% of the beams' flexural capacity. One beam was fully damaged by preloading to failure and repaired before strengthening by replacing the crushed concrete. The data showed that the pre-damaged strengthened beams exhibited ultimate capacities up to 8% lower than those of the undamaged strengthened beams. However, the load carrying capacities of pre-damaged strengthened beams were more than those predicted by ACI 440 design guide, fib Bulletin 14, and JSCE design recommendations. Both fib Bulletin 14 and JSCE design recommendations gave very conservative predictions with average ratios of experimental to predicted ultimate capacity of 2.02 and 2.35, respectively. More accurate predictions were obtained by ACI 440 design guide as the corresponding ratio was 1.24. These results indicate that strong confidence and reliability can be placed in applying CFRP strengthening to structurally damaged WSBs.

Keywords

CFRP reinforcement; Concrete beams; Strengthening; Structural damage; debonding.

Rajeh A. Al-Zaid [a]
Ahmed K. El-Sayed [b]
Abdulaziz I. Al-Negheimish [c]
Ahmed B. Shuraim [d]
Abdulrahman M. Alhozaimy [e]

[a]Professor, Department of Civil Engineering, King Saud University, Riyadh, Saudi Arabia, E-mail: rajehalzaid@hotmail.com
[b]Assistant Professor, Center of Excellence for Concrete Research and Testing, King Saud University, Riyadh, Saudi Arabia, E-mail: ahelsayed@ksu.edu.sa. On leave from Housing and Building National Research Center, Giza, Egypt.
[c]Associate Professor, Department of Civil Engineering, King Saud University, Riyadh, Saudi Arabia, E-mail: negaimsh@ksu.edu.sa
[d]Professor, Department of Civil Engineering, King Saud University, Riyadh, Saudi Arabia, E-mail: ashuraim@ksu.edu.sa
[e]Professor, Department of Civil Engineering, King Saud University, Riyadh, Saudi Arabia. E-mail: alhozimy@ksu.edu.sa

1 INTRODUCTION

The joist-banded floor system is one of the popular floor systems used in building construction particularly in the Middle East. The system is characterized by having joists in one direction supported by wide shallow beams (WSBs) or bands that have the same thickness as the joists (Shuraim and Al-Negheimish, 2011). There are a large number of concrete buildings across the region that were constructed using this floor system and are structurally deficient by today's standards. In order to preserve these structures, strengthening and repair are considered essential to maintain their structural integrity and to increase public safety.

The use of carbon fiber reinforced polymer (CFRP) for external strengthening by adhesively bonding to reinforced concrete (RC) structures has become a popular retrofit technique. The use of such technique for flexural strengthening of RC beams has proven to be effective in enhancing both strength and stiffness. The main problem associated with this technique is the premature failure which occurs in a brittle and sudden manner due to debonding between CFRP and concrete substrate before utilizing the full strength of the strengthening area. The premature failure modes include plate end debonding/concrete cover separation; critical diagonal crack debonding; and intermediate crack induced debonding (IC debonding). IC debonding is considered to be a more dominant failure mode compared to other debonding failure modes (Liu et al., 2007). Several studies (Rahimi and Hutchinson, 2001; Shahawy et al., 2001; Bencardino et al., 2002; Rabinovitch and Frostig, 2003; Teng et al., 2003; Yao et al. 2004; Liu et al., 2007; Rosenboom and Rizkalla, 2008; Aram et al., 2008) attributed the occurrence of IC debonding to the stress concentrations due to the opening of flexural cracks which are typically larger than the stress concentrations at the plate end, and hence debonding advances from the intermediate cracks towards the support, as illustrated in Figure 1. Rosenboom and Rizkalla (2008) indicated that this mode of failure is common in structures with (1) high shear span-to-depth ratio; (2) FRP strengthening with low axial stiffness per unit width; (3) strengthening plate termination in regions near the support; or (4) anchorage details.

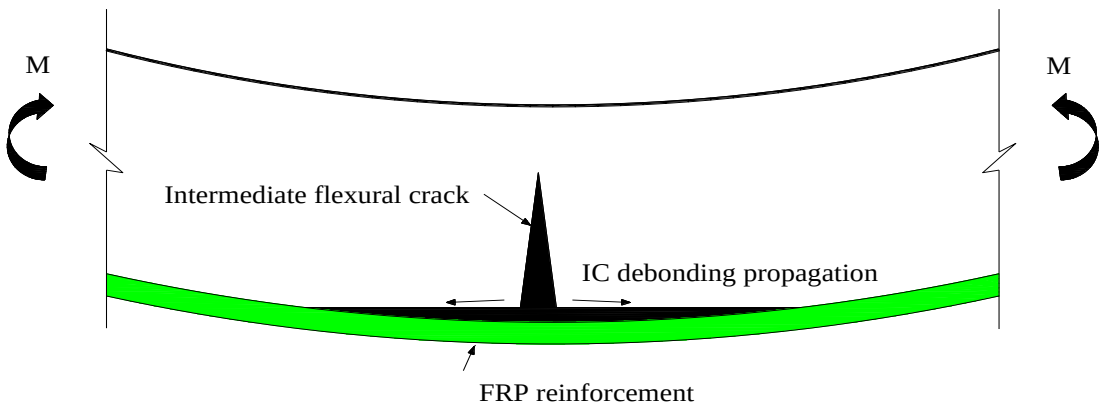

Figure 1: IC debonding mechanism [Liu et al., 2007].

Most of the research work available in the literature on CFRP-strengthened beams has been done on virgin beams while concrete structures which need repair and strengthening in real life already underwent different levels of cracking and damage. The existing cracks may influence the efficiency of FRP strengthening particularly for IC debonding-critical members. Even the limited work in the literature on structurally damaged beams that have been previously loaded to proportions of their ultimate strength and are consequently cracked, has been done on beams preloaded to 30-70% of their flexural capacities. It is to the best knowledge of the authors; no work has been done to examine the efficiency of CFRP strengthening for beams preloaded to higher loads that represent the situation when the beam is overloaded and consequently substantially cracked. Arduini and Nanni (1997) strengthened number of beams preloaded prior to the application of CFRP sheets. The applied load was equal to 30% of the nominal capacity of the beams. Arduini and Nanni (1997) indicated that this load level was intended to simulate a reasonable service condition and allowed the formation of three to four cracks in the region of constant moment. Some of the pre-damaged beams were strengthened in the unloaded state and some beams were strengthened under sustaining load. The results showed that the performance of strengthened pre-damaged beams was not significantly different from strengthened original undamaged beams. These results were also confirmed by the findings of Shin and Lee (2003) through examining experimentally the effect of

sustaining load at strengthening on the flexural behavior of CFRP-strengthened beams. The level of sustaining load at the time of strengthening was 50 and 70% of the nominal flexural strength of the beams. The results showed that the load-carrying capacities of strengthened beams at different levels of sustaining load were almost the same as those of strengthened virgin beams. Liu et al. (2007) described a numerical model that simulates the IC debonding behavior of plated RC beams based on partial interaction theory. The model was used to examine the effects of flexural cracking on the behavior of FRP-strengthened beams by varying the crack spacings and the number of cracks along the beams. It was shown that a lower bound to the debonding strain is a beam with single flexural crack and that the debonding strain can be significantly increased when there is increasing number of flexural cracks. Substantial increase in debonding strain can also occur as the crack spacing reduces. Jayaprakash et al. (2011) investigated the effect of CFRP longitudinal strengthening on the flexural capacity of prestressed beams pre-damaged before strengthening. The experimental results showed that the flexural capacity of the repaired beams increased to a maximum enhancement of 172.4% over the unstrengthened beam. Further, the comparison between the experimental and theoretical capacities showed good agreement.

To build confidence in the efficiency of CFRP system for repairing and strengthening of RC structures with WSBs, an extensive research program is being undertaken at King Saud University on both isolated beams and proto-type existing structure. The experimental performance of full-scale isolated WSBs as affected by the area, configuration, type, and modulus of elasticity of CFRP reinforcement has been investigated and presented elsewhere (Al-Negheimish et al., 2012). In addition, a simple numerical model for predicting the structural behavior of RC beams strengthened for flexure with externally bonded FRP reinforcement has been developed and presented elsewhere (Al-Zaid et al., 2012). Due to its large span-to-depth ratio, a WSB strengthened with CFRP is more susceptible to generate IC debonding failure mode under loading and the existing cracks prior to strengthening may affect this mode of failure as well as the efficiency of CFRP strengthening. This paper investigates the effect of structural damaging on the effectiveness of CFRP strengthening of WSBs beams. The beams were pre-damaged by preloading to different load levels up to 95% of the flexural capacity of the beams. The study was extended to include a beam fully damaged by preloading to the failure load then repaired before CFRP strengthening by replacing the concrete in the heavily damaged portion of the beam. The load carrying capacities of the strengthened beams were analyzed using the design codes and guidelines pertaining to FRP strengthening.

2 EXPERIMENTAL INVESTIGATION

2.1 Materials

The CFRP reinforcement used in this study was pultruded plates having a width of 120 mm and a thickness of 1.4 mm. The tensile strength and modulus of elasticity as provided by the manufacturer were 2800 MPa and 165 GPa, respectively (Sika carboDur plates, 2009). The adhesive used to bond the CFRP plates to the concrete beams was a thixotropic, structural two-component adhesive, based on a combination of epoxy resins and special fillers. The elastic modulus and bond strength of the adhesive were 12.8 GPa and 4 MPa, respectively, as provided by the manufacturer (Sikadur-30, 2009).

Deformed steel bars of 16 mm diameter were used as main tensile reinforcement while deformed steel bars of 12 mm diameter were used as top reinforcement. The stirrups used were deformed steel bars having a diameter of 8 mm. The actual tensile properties of the 16 and 12 mm diameter bars were determined using standard tensile tests performed on three samples of each bar size. The average yield strengths of the bars were 562 and 533 MPa, respectively. The corresponding moduli of elasticity were 205 and 207 GPa.

The beams were constructed using normal weight concrete provided by a local ready-mix supplier. Concrete cylinders 150 × 300 mm were cast during casting the beams and cured under the same conditions as the beams. The average compressive strength at the time of beam testing was 30 MPa based on cylinder tests.

2.2 Test specimens

A total of 8 full-scale reinforced concrete beams were constructed and tested up to failure. The beams measured 5300 mm long, 500 mm wide, and 250 mm deep. Figure 2 shows the typical reinforcement details of the test beams. The dimensions and reinforcement of the beams were designed to reflect the common dimensions and reinforcement of such beams in real structures (Shuraim and Al-Negheimish, 2011). Seven beams were strengthened using CFRP plates bonded to the tension faces of the beams, while one beam was unstrengthened and served as control. The test variables were the preloading level before plating and the reinforcement ratio of the external CFRP reinforcement.

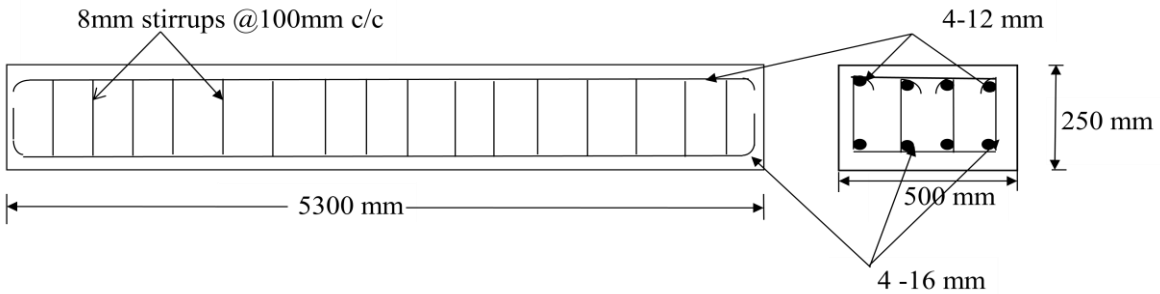

Figure 2: Reinforcement details of the test beams.

Table 1 summarizes the strengthening details of the test beams while Figure 3 presents the typical strengthening schemes. The designation of the beams can be explained as follows. The control beam which has no external reinforcement is referred to as C. For strengthened beams, the letter B stands for beam, the first number (0.3 or 0.6) indicates the reinforcement ratio of the external reinforcement (ρ_f), the second number (0, 0.3, 0.5, 0.9, or 1) indicates the preloading level as a ratio of the ultimate capacity of the control beam, $M_{u\ contr}$. The letter R stands for the repairing before CFRP strengthening. Each strengthened beam was provided with one layer of CFRP plates with a length of 4800 mm and a width of 240 or 480 mm for beams of $\rho_f = 0.32$ or 0.63 %, respectively as shown in Figure 3.

As given in Table 1, beam B-0.6-0.3 was preloaded to 0.35 $M_{u\ contr}$ whereas beams B-0.6-0.5 and B-0.3-0.5 were preloaded to 0.55 $M_{u\ contr}$, representing the range of service loading in real structures while beam B-0.6-0.9 was preloaded to 0.95 $M_{u\ contr}$ representing the situation when the beam is overloaded. All of these four beams were strengthened in the unloaded state after removing the preload. Beam B-0.6-1R was preloaded to the failure load, $M_{u\ contr}$, then repaired and strengthened with CFRP plates. The preloading was applied using the same configuration of the test to failure (Figure 3). Beams B-0.6-0 and B-0.3-0 were strengthened without preloading.

Table 1: Details of test beams.

Beam	External CFRP reinforcement			Preloading level before strengthening	Remarks
	Thickness (mm)	Width (mm)	Reinforcement ratio, ρ_f (%)		
C	--	--	--	--	Control
B-0.6-0		480	0.63	0	Strengthened without preloading
B-0.6-0.3		480	0.63	0.35 $M_{u\ contr}$	Strengthened after preloading and releasing the load
B-0.6-0.5		480	0.63	0.55 $M_{u\ contr}$	
B-0.6-0.9		480	0.63	0.95 $M_{u\ contr}$	
B-0.6-1R	1.4	480	0.63	$M_{u\ contr}$	Preloaded to failure, repaired, and strengthened
B-0.3-0		240	0.32	0	Strengthened without preloading
B-0.3-0.5		240	0.32	0.55 $M_{u\ contr}$	Strengthened after preloading and releasing the load

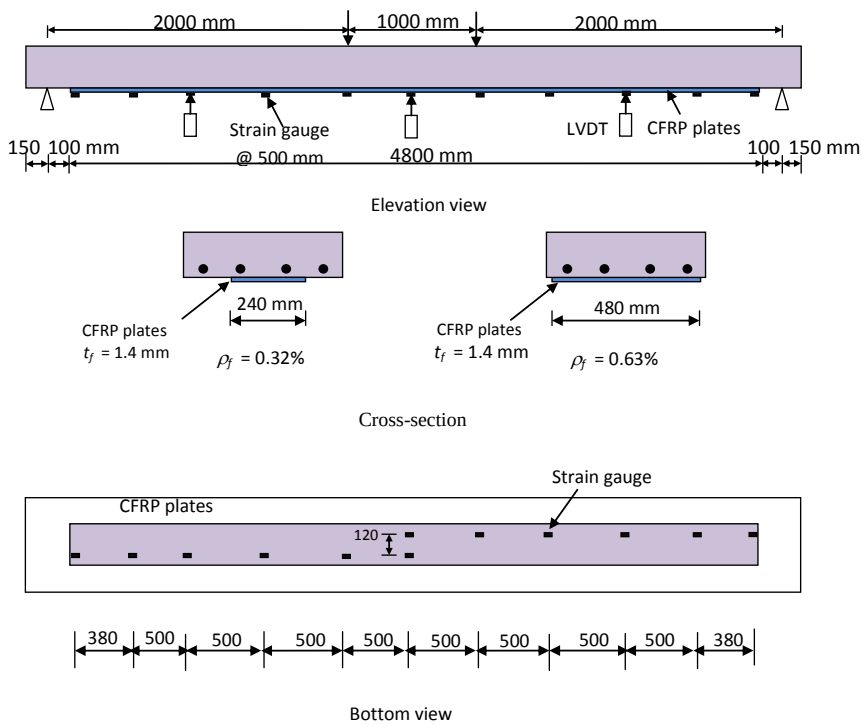

Figure 3: Typical strengthening schemes and test setup.

2.3 Repairing of fully damaged beam

Beam B-0.6-1R was preloaded up to failure and consequently underwent severe damage which was characterized by substantial cracking, deformation, and crushing of the concrete in the constant moment zone. Prior to strengthening with CFRP plates, the beam was repaired according to the following steps. The first step was recovering almost the entire midspan deflection of the beam which was achieved by loading the beam with the same setup used for preloading but after turning the beam over where the top surface of the beam in this stage was the bottom one during the preloading stage. The second step was removing the crushed concrete and heavily cracked

concrete in the constant moment zone. The concrete within the zone of 0.6 m from the centerline of the beam for each side was entirely removed. Before placing the new concrete which had the same properties as the old one and provided by the same supplier, the contact surface of the old concrete was coated with bonding agent to ensure full bond between the old and new concrete. Figure 4 shows the repaired portion of the beam and illustrates the beam during placing the repair concrete. The beam was strengthened with CFRP plates after 28 days of pouring the repair concrete.

2.4 Strengthening procedure

The CFRP plates were cut to the required length (4800 mm) for strengthening the concrete beams. Special consideration was given to the surface preparation before bonding the CFRP plates to the concrete surface. Sandblasting was employed to remove the weak surface layer from the concrete beams and then the surface was cleaned with a high-pressure air jet and the CFRP plates were bonded to the concrete surface using the epoxy adhesive. The epoxy adhesive was applied to the CFRP plates and to the marked locations on the concrete surface. Then, the strips were pressed onto the concrete substrate using a small roller. Excess adhesive was squeezed out the sides and removed; this ensured that any trapped air was removed. After the entire application process was completed the overall thickness of adhesive ranged between 2-3 mm. The epoxy adhesive was then allowed to cure in the laboratory environment for seven days before testing.

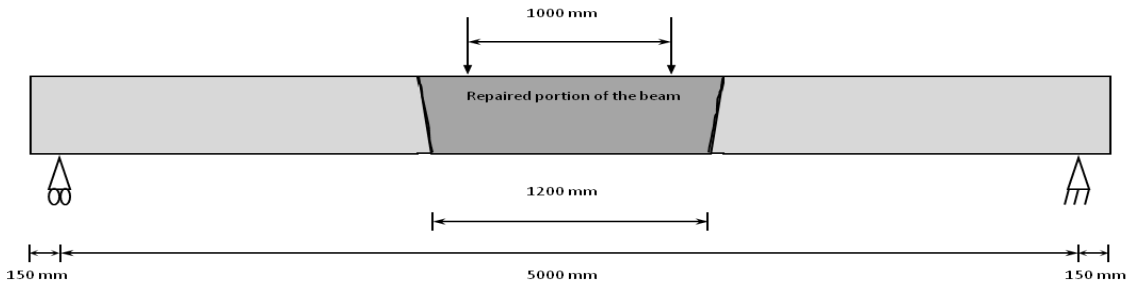

(a) Repaired portion of the beam

(b) Placing of the repair concrete

Figure 4: Repairing of the fully damaged beam (B-0.6-1R).

2.4 Test setup and instrumentation

The beams were tested in four-point bending over a simply-supported span of 5000 mm and a shear span of 2000 mm, as shown in Figure 3. A 500 kN actuator was used to apply the load. For each beam, electrical resistance strain gauges were bonded to the reinforcing steel, CFRP reinforcement, and concrete at various locations along the length of the beam. The deflection at mid-span was measured using two LVDTs at each side of the beam while one LVDT was used at each mid-shear span to monitor the deflection profile along the beam. Two high-accuracy LVDTs (± 0.001 mm) were installed at positions of first cracks to measure crack width at the level of tension steel.

During testing, load was monotonically applied at a stroke-controlled rate of 1.0 mm/min. The loading was stopped when the first two cracks appeared and the initial crack widths were measured manually using a hand-held 50X microscope. Then, the two high-accuracy LVDTs were installed to measure crack width with increasing load. The applied load, displacements, crack widths, and strain readings were electronically recorded during the test using a data acquisition system.

3 TEST RESULTS AND DISCUSSION

For the pre-damaged beams and at the specified preloading level, the maximum crack widths measured at the constant moment zone ranged between 0.17 and 0.35 mm. After unloading, however, the cracks were partially closed and the maximum crack widths ranged between 0.04 and 0.09 mm. Figure 5 shows the crack patterns of the beams after preloading indicating that the number and depth of the cracks increase with the increase of preloading level. After CFRP strengthening, the beams were tested up to failure. Table 2 summarizes the test results of the beams. It should be noted that the yield and failure moments given in Table 2 include the bending moment at mid-span due to the self-weight of the beam, which equals 9.4 kN.m.

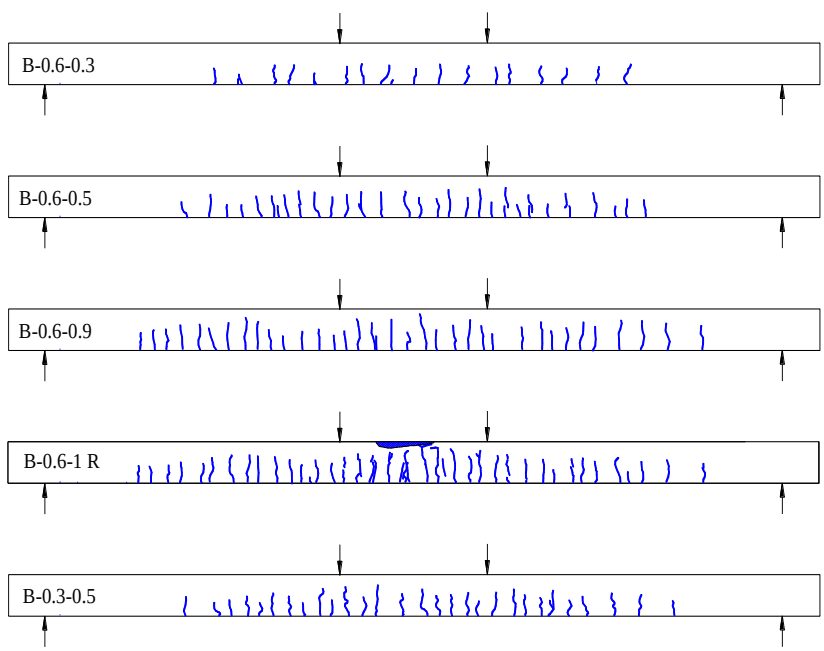

Figure 5: Crack patterns of the damaged beams due to preloading and before strengthening.

3.1 Deflection response

The applied moment-midspan deflection curves of the test beams are plotted in Figure 6. The moment-deflection curve of the control beam, C, indicates the typical relationship which is characterized by tri-linear behavior. Beams B-0.6-0 and B-0.3-0 strengthened without preloading showed also a tri-linear behavior but in the postyielding phase up to failure, the beams did not exhibit yielding plateau indicating less ductile behavior. It is interesting to note that, even though extensively cracked prior to reloading, pre-damaged strengthened beams exhibited comparable or slightly increased flexural stiffness in comparison to the postcracking flexural stiffness of their counterparts strengthened without preloading. Based on this result, it can be concluded that preloading of the beams has no effect on the postcracking flexural stiffness of the strengthened beams.

Table 2: Summary of test results.

Beam	Yield moment*, M_y (kNm)	Failure moment*, M_u (kNm)	Mid-span deflection (mm) at		Crack width (mm) at		Max. strain ($\mu\varepsilon$)			Mode of failure+
			Yield δ_y	Failure δ_u	Yield w_y	Failure w_u	Steel	CFRP	Concrete	
C	89.4	98.4	45	175	0.48	4.68	21104	--	-3417	Y-C
B-0.6-0	178.8	253.8	53	101	0.24	0.46	17654	6523	-2829	Y-IC
B-0.6-0.3	184.4	236.8	57	92	0.26	0.42	13123	6661	-3742	Y-IC
B-0.6-0.5	178.9	240.7	54.4	92	0.29	0.47	14513	6000	-3073	Y-IC
B-0.6-0.9	176.6	233.7	50.1	91.3	0.31	0.51	16815	6023	-2981	Y-IC
B-0.6-1R	180.0	252.4	51.5	80.7	0.22	0.42	--	5350	-2757	Y-IC
B-0.3-0	122.0	174.2	43	77	0.35	0.74	25618	6367	-2542	Y-IC
B-0.3-0.5	122.2	177.0	38.9	75.1	0.35	0.81	27014	6423	-2495	Y-IC

* including the effect of self-weight. + Y-C = yielding of reinforcing steel followed by concrete crushing, Y-IC = yielding of reinforcing steel followed by intermediate crack-induced debonding (IC debonding).

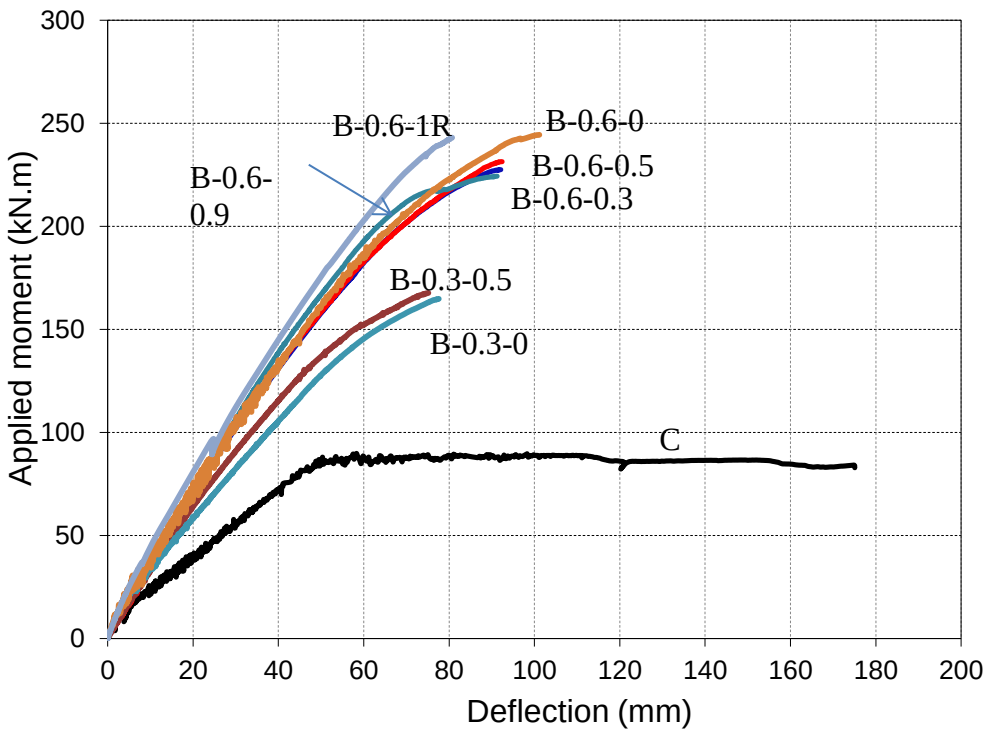

Figure 6: Applied moment-deflection response.

3.2 Cracking behavior and modes of failure

For all beams and at early load levels, crack formation was initiated in the flexural span between the two concentrated loads where the flexural stress is highest and shear stress is zero. The cracks were vertical cracks perpendicular to the direction of the maximum principal tensile stress induced by pure bending. For the control beam, first crack occurred at applied moment of 9 kN.m, while first cracks for beams B-0.6-0 and B-0.3-0 occurred at applied moments of 21 and 17 kN.m, respectively. As load increased, additional cracks developed within the shear span.

Table 2 gives the modes of failure of the tested beams. Beam C failed by crushing of the concrete at the constant moment zone after extensive yielding of the tensile steel. All strengthened beams experienced the same mode of failure which was delamination of the CFRP reinforcement by intermediate crack (IC) debonding that started in the vicinity of the mid-span of the beam and propagated towards support. The failure occurred at the FRP-concrete interface in the concrete surface layer which was evidenced by a thin layer of concrete attached to the plates after delamination. The cracking patterns of CFRP-strengthened beams at failure are shown in Figure 7. Beams of the same ρ_f showed similar cracking characteristics in terms of crack spacing and numbers. Typical failure modes of the test beams are illustrated in Figure 8.

Figure 9 presents the variation of the widths of the first crack with the applied moment for the test beams. It should be pointed out that the crack width measurements for preloaded beams started at the beginning of reloading and the LVDTs for measuring crack widths were installed at the first two cracks appeared during the preloading stage. The figure shows that increasing the amount of CFRP reinforcement increases the efficiency of CFRP reinforcement in restricting the opening of the crack width. The figure also indicates that preloaded beams with $\rho_f = 0.63\%$ experienced moment-crack width relationships similar to that of beam B-0.6-0 strengthened without preloading. The same finding can be observed for beams B-0.3-0.5 and B-0.3-0 with $\rho_f = 0.32\%$. Thus, it is evident that the efficiency of CFRP strengthening in restricting the crack opening has not been affected by pre-cracking.

3.3 Strains in reinforcement and concrete

From the continuous monitoring of strain gauges attached to the CFRP reinforcement, the strain profiles along the length of the beams were plotted at various load levels. Figure 10 shows the CFRP strain profile of two selected beams: beam B-0.6-0.3 and beam B-0.3-0.5. As expected, the CFRP strain along the length of the beam followed the profile of bending moment by increasing towards midspan. The variation of CFRP strains measured at midspan of the beams with the applied moments is plotted in Figure 11. The beams strengthened with the same ρ_f showed approximately similar performance irrespective of the preloading level. However, beams B-0.3-0 and B-0.3-0.5 strengthened with $\rho_f = 0.32\%$ experienced more CFRP strain at the same loading level in comparison to the beams of $\rho_f = 0.63\%$. The moment-CFRP strain relationship appears to be trilinear for beams B-0.6-0 and B-0.3-0 strengthened without preloading and bilinear for the other preloaded beams. A significant change of the slopes of the curves occurred after yielding of internal steel indicating that the CFRP plates start to take over any load increment applied to the beam after steel yielding. Figure 11 and Table 2 indicate that the debonding strain, ε_{fd}, was not affected by pre-cracking as the pre-cracked strengthened beams exhibited approximately similar ε_{fd} to that of their counterparts strengthened without preloading. It is also interesting to observe that beams strengthened with $\rho_f = 0.32\%$ failed at almost the same ε_{fd} as of beams strengthened with $\rho_f = 0.63\%$, indicating that the width of CFRP plates has no effect on ε_{fd}. The measured ε_{fd} for beams B-0.3-0 and B-0.3-0.5 with $\rho_f = 0.32\%$ were 6,367 and 6,423 $\mu\varepsilon$, respectively, which is in the same range of 6,000 to 6661 $\mu\varepsilon$ for beams strengthened with $\rho_f = 0.63\%$ except for beam B-0.6-1R which showed relatively lower value of ε_{fd} (5,350 $\mu\varepsilon$), as given in Table 2. In comparison to

the rupture strain, these measured strains of the CFRP plates at failure were in the range of 31-39% of the rupture strain (17,000$\mu\varepsilon$).

Table 2 gives also the measured midspan strains in the reinforcing steel and concrete for each beam at failure. The maximum steel tensile strain ranged between 13,123 and 17,654$\mu\varepsilon$ for beams with $\rho_f = 0.63\%$ and the corresponding range for beams of $\rho_f = 0.32\%$ was 25618 to 27014$\mu\varepsilon$. The concrete compressive strain measured at failure for the strengthened beams ranged between 2829 and 3742 $\mu\varepsilon$ for beams with $\rho_f = 0.63\%$ and ranged from 2495 to 2542 $\mu\varepsilon$ for beams with $\rho_f = 0.32\%$, indicating that the compressive strength of the concrete was not fully utilized for most of the beams.

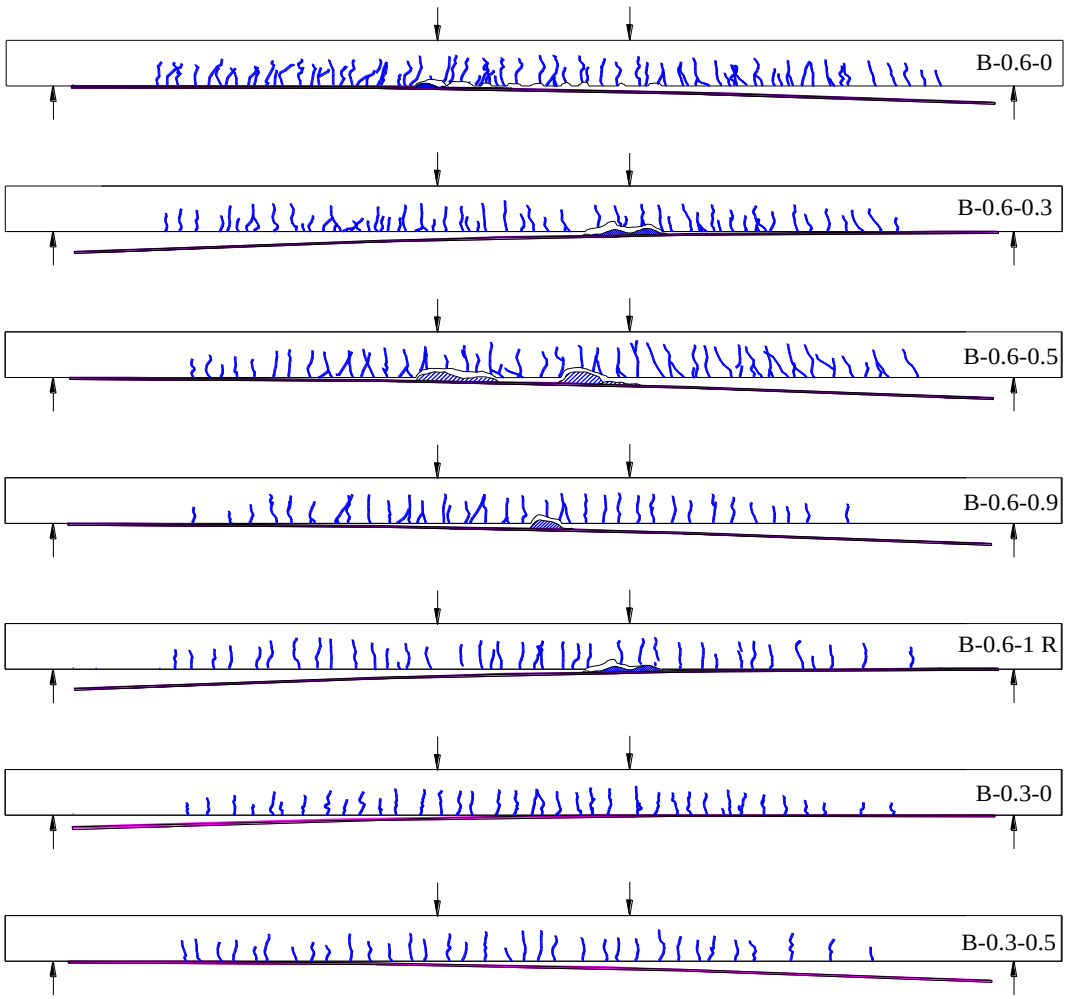

Figure 7: Cracking patterns of the strengthened beams at failure.

3.4 Ultimate capacities

The ultimate moment and yield capacities of the test beams are given in Table 2. It can be noticed that all strengthened beams showed higher ultimate capacities with respect to the control beam. Beams B-0.3-0 and B-0.3-0.5 strengthened with $\rho_f = 0.32\%$, showed increases in ultimate capacities of 77 and 80%, respectively. On the other hand, the increase in ultimate capacity ranged between 138 and 158% for the beams strengthened with $\rho_f = 0.63\%$.

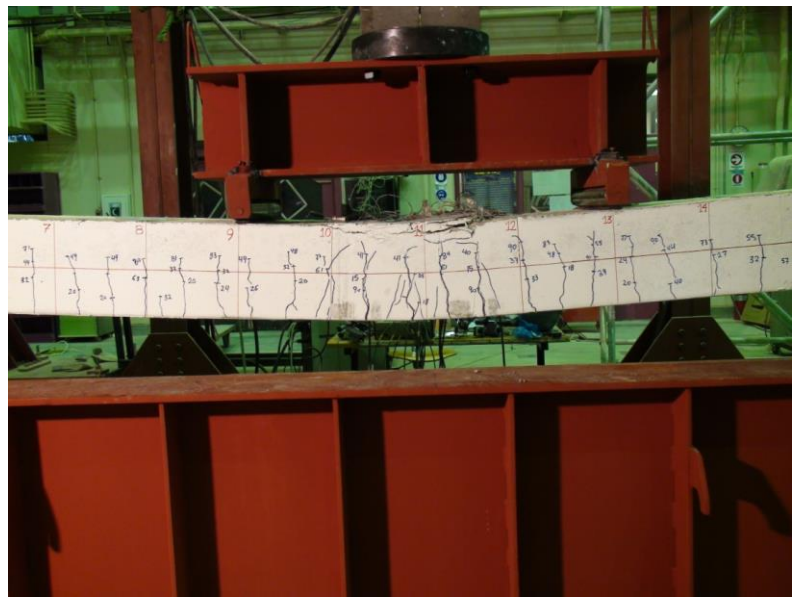

(a) Flexural concrete crushing (beam C)

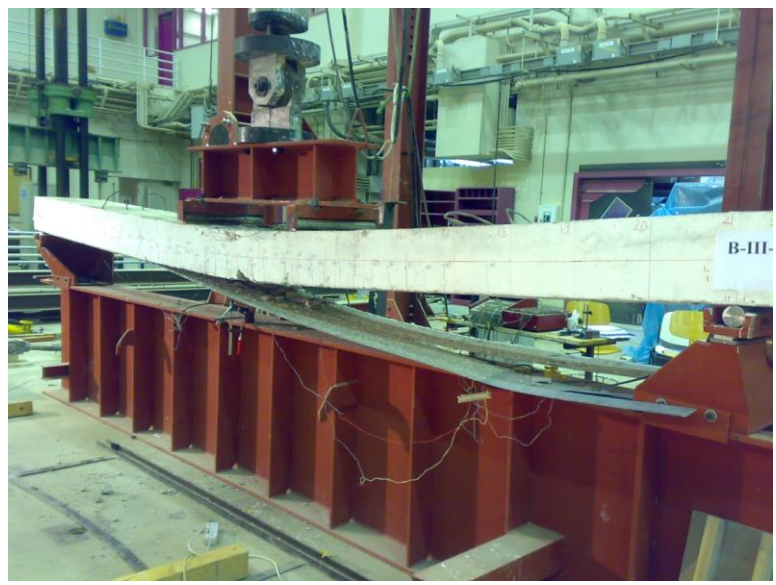

(b) Typical IC debonding failure mode (beam B-0.6-0.9)

Figure 8: Modes of failure.

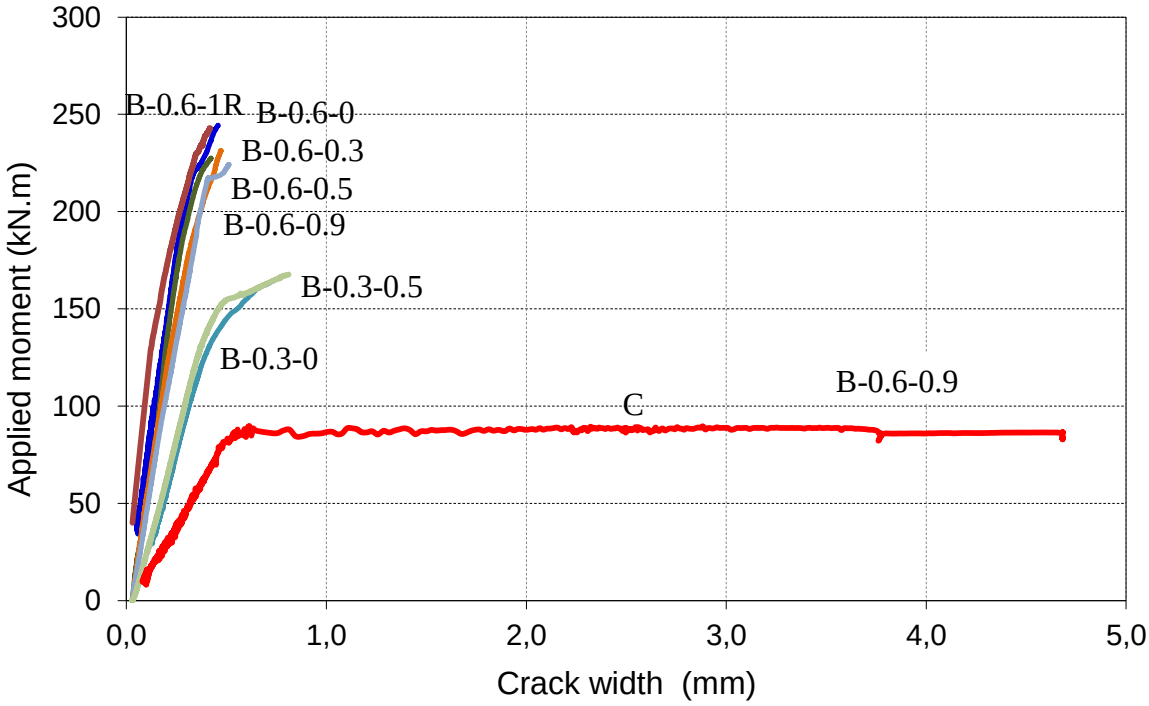

Figure 9: Applied moment-crack width relationship.

The test results indicate that the four beams B-0.6-0.3, B-0.6-0.5, B-0.6-0.9 and B-0.6-1R strengthened with the same amount of CFRP reinforcement experienced similar ultimate capacities in the range of 233.7 and 252.4 kN.m showing differences less than 8%. Comparing the ultimate capacities of these four beams with that of beam B-0.6-0 strengthened without preloading, it can be observed that the four beams showed only 1-8% lower capacities than that of beam B-0.6-0 with the repaired beam B-0.6-1R giving almost comparable capacity to beam B-0.6-0. Similarly, beam B-0.3-0.5 showed almost the same capacity as that of beam B-0.3-0 strengthened without preloading. Although IC debonding mode of failure developed by all strengthened beams in this study is believed to be initiated due to the stress concentrations caused by the widening of flexural cracks, the CFRP debonding strain and consequently the ultimate capacity of the strengthened beams has not been significantly affected by pre-cracking. This can be attributed to the fact that the beams were strengthened at the unloaded stage after removing the preload and the maximum crack widths measured at this stage were relatively small (less than 0.09 mm). The authors believe that the crack width at the time of strengthening is of prime importance rather than the number of cracks. The pre-cracked beams showed several cracks before strengthening due to preloading (Figure 5) but the widths of these cracks were significantly reduced after removing the loads. Further, the introduction of CFRP reinforcement helped to restrict the opening of these cracks under loading and finally all strengthened beams had approximately similar cracking patterns at failure (Figure 7) even though they had different cracking patterns before strengthening.

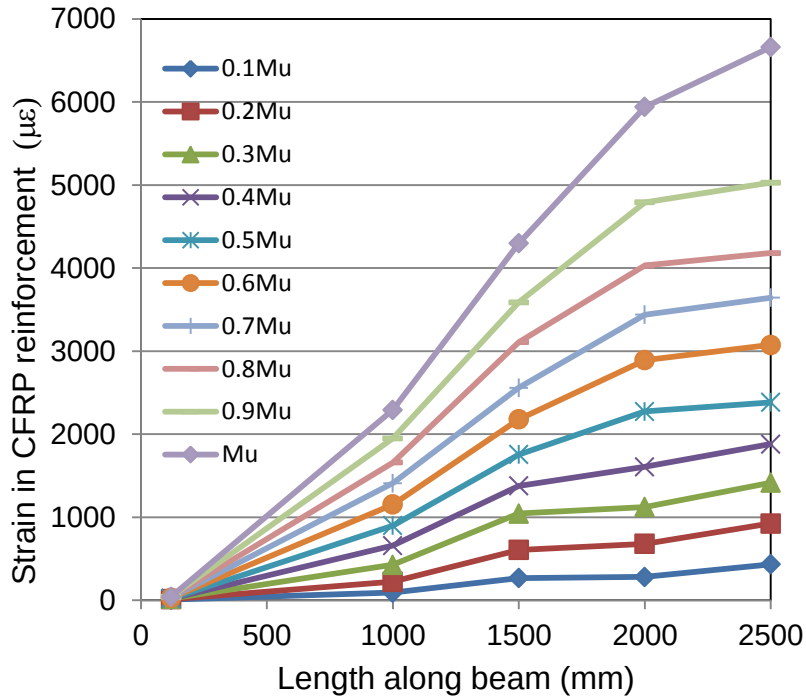

(a) Beam B-0.6-0.3

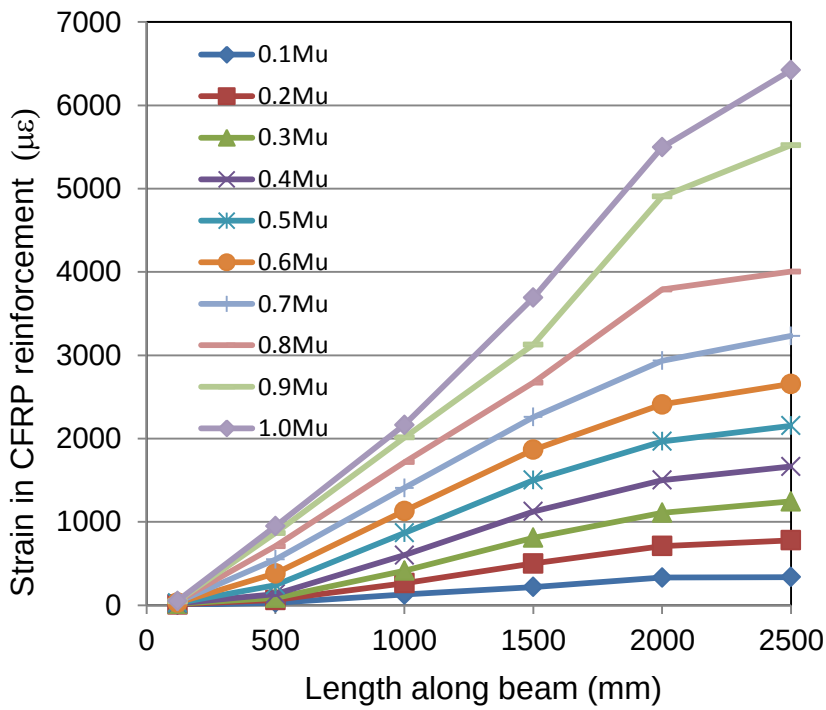

(b) Beam B-0.3-0.5

Figure 10: CFRP strain profile.

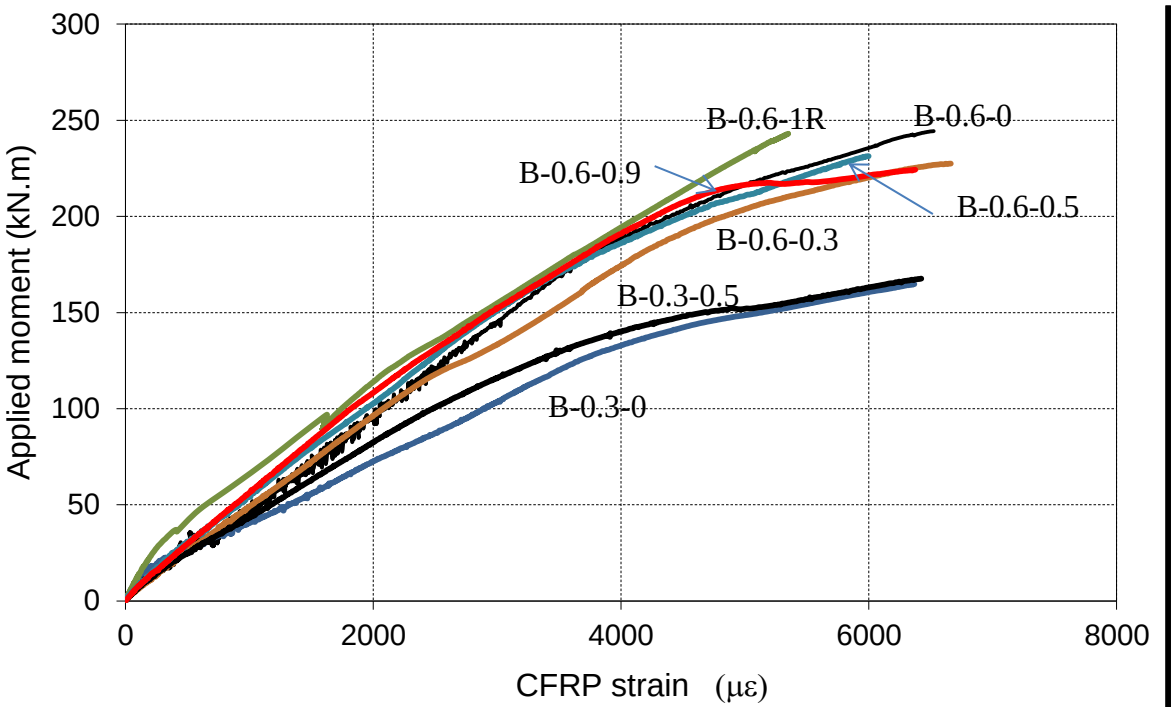

Figure 11: Applied moment-CFRP strain relationship.

4 EXPERIMENTAL RESULTS VERSUS THEORETICAL PREDICTIONS

4.1 ACI 440.2R-08

ACI Committee 440 in its document, ACI 440.2R-08 (2008), recommends a limiting value for the usable ultimate strain of FRP laminates to prevent the occurrence of IC debonding failure as given by Eq. (1). This implies that the ultimate moment capacity is primarily controlled by the debonding strain rather than by the ultimate rupture strain of FRP laminates.

$$\varepsilon_{fd} = 0.41\sqrt{\frac{f_c^{'}}{nE_f t_f}} \leq 0.9\varepsilon_{fu} \qquad (1)$$

where $f_c^{'}$ is the concrete compressive strength, n is the number of FRP plies, E_f is the modulus of elasticity of FRP, t_f is the thickness of one ply of FRP, and ε_{fu} is the design rupture strain of FRP reinforcement.

Eq. (1) was used to calculate the debonding strain ε_{fd} of the test beams considering the properties of the CFRP reinforcement and the concrete compressive strength used in this investigation. The calculated values are given in Table 3. It can be seen that Eq. (1) gives reasonable conservative predictions for all tested beams including the pre-cracked beams. The average $\varepsilon_{fd\ exp}/\varepsilon_{fd\ ACI}$ ratio for all tested beams was 1.33 with a coefficient of variation of 7%.

The ultimate strength of the strengthened reinforced concrete section can be calculated by applying the strain compatibility method and equilibrium equations considering the debonding strain, ε_{fd}, determined from Eq. (1) according to the following equation:

$$M_u = A_s f_s\left(d - \frac{\beta_1 c}{2}\right) + \psi_f A_f \varepsilon_{fd}\left(h - \frac{\beta_1 c}{2}\right) + A_s^{'} f_s^{'}\left(\frac{\beta_1 c}{2} - d^{'}\right) \quad (2)$$

where A_s and $A_s^{'}$ are the areas of tensile and compressive steel reinforcement, respectively; f_s and $f_s^{'}$ are the respective stresses; d and $d^{'}$ are the distances from extreme compression fiber to centroids of tensile and compressive steel reinforcement, respectively; A_f is the area of FRP reinforcement; h is the overall height of the beam; c is the distance from extreme compression fiber to the neutral axis; β_1 is the ratio of depth of equivalent rectangular stress block to depth of the neutral axis; and ψ_f is a reduction factor of 0.85 recommended by ACI 440 Committee to account for uncertainties inherent in FRP.

The calculated ultimate capacities of the CFRP-strengthened beams according to Eq. (2) together with the experimental results are given in Table 3. It should be pointed out that the reduction factor ψ_f was set to equal one in the calculations. The comparison between the experimental and calculated capacities shows that the ACI 440 method provides reasonable conservative predictions for the moment capacities of all test beams including the pre-cracked beams as the average ratio of the experimental to calculated capacities was 1.24 with a coefficient of variation of 3%.

4.2 fib Bulletin 14

The Fédération Internationale du Béton (*fib*) *Bulletin 14* (2001) recommends a design equation for evaluating the debonding strain ε_{fd} based on fracture mechanics approach similar to that recommended by the Concrete Society-Technical Report 55 (2004). According to *fib Bulletin 14* (2001), the debonding strain ε_{fd} can be calculated as follows for FRP bond lengths $l_b \geq l_{b,\,max}$:

$$\varepsilon_{fd} = \alpha c_1 k_c k_b \sqrt{\frac{f_{ct}}{n E_f t_f}} \quad (3a)$$

while for $l_b < l_{b,\,max}$, ε_{fd} is given by:

$$\varepsilon_{fd} = \alpha c_1 k_c k_b \sqrt{\frac{f_{ct}}{n E_f t_f}} \frac{l_b}{l_{b,\max}}\left(2 - \frac{l_b}{l_{b,\max}}\right) \quad (3b)$$

$$l_{b,\max} = \sqrt{\frac{n E_f t_f}{c_2 f_{ct}}} \quad (4)$$

where α is a reduction factor accounting for the influence of inclined cracks on the bond strength ($\alpha = 1$ for beams with sufficient internal and external shear reinforcement and for slabs, otherwise $\alpha = 0.9$); c_1 and c_2 can be obtained through calibration with test results or can be taken 0.64 and 2.0, respectively, for CFRP strips; k_c is a factor accounting for the state of compaction of concrete (k_c can generally be assumed to be equal to 1.0, but for FRP bonded to concrete faces with low compaction, e.g. faces not in contact with the formwork during casting, $k_c = 0.67$); f_{ct} is the tensile strength of concrete; and k_b is a geometry factor:

$$k_b = 1.06\sqrt{\frac{2 - \frac{b_f}{b}}{1 + \frac{b_f}{400}}} \quad (5)$$

where b_f is the width of FRP and $b_f/b \geq 0.33$.

Table 3: Comparison of experimental and predicted results.

Beam	Experimental		ACI 440 (2008) calculations				*fib Bulletin 14 (2001)* calculations				JSCE (1997) calculations			
	$\varepsilon_{fd\ exp}$ ($\mu\varepsilon$)	$M_{u\ exp}$ (kN.m)	$\varepsilon_{fd\ ACI}$ ($\mu\varepsilon$)	$M_{u\ ACI}$ (kN.m)	$\varepsilon_{fd\ exp}/\varepsilon_{fd\ ACI}$	$M_{u\ exp}/M_{u\ ACI}$	$\varepsilon_{fd\ fib}$ ($\mu\varepsilon$)	$M_{u\ fib}$ (kN.m)	$\varepsilon_{fd\ exp}/\varepsilon_{fd\ fib}$	$M_{u\ exp}/M_{u\ fib}$	$\varepsilon_{fd\ JSCE}$ ($\mu\varepsilon$)	$M_{u\ JSCE}$ (kN.m)	$\varepsilon_{fd\ exp}/\varepsilon_{fd\ JSCE}$	$M_{u\ exp}/M_{u\ JSCE}$
B-0.6-0	6523	253.8	4672	196	1.40	1.29	2413	117	2.70	2.17	2081	101.8	3.13	2.49
B-0.6-0.3	6661	236.8	4672	196	1.43	1.21	2413	117	2.76	2.02	2081	101.8	3.20	2.33
B-0.6-0.5	6000	240.7	4672	196	1.28	1.23	2413	117	2.48	2.05	2081	101.8	2.88	2.36
B-0.6-0.9	6023	233.7	4672	196	1.29	1.19	2413	117	2.50	2.00	2081	101.8	2.89	2.30
B-0.6-1R	5350	252.4	4672	196	1.15	1.28	2413	117	2.22	2.16	2081	101.8	2.57	2.48
B-0.3-0.0	6367	174.2	4672	142	1.36	1.23	2494	93	2.55	1.87	2081	78.2	3.06	2.23
B-0.3-0.5	6423	177.0	4672	142	1.37	1.25	2494	93	2.57	1.90	2081	78.2	3.09	2.26
Mean					**1.33**	**1.24**			**2.54**	**2.02**			**2.98**	**2.35**
Standard deviation					**0.09**	**0.04**			**0.17**	**0.12**			**0.21**	**0.10**
Coefficient of variation (%)					**7**	**3**			**7**	**6**			**7**	**4**

Table 3 shows the comparison between the predicted debonding strains of the test beams using Eq. (3) and the experimental results. The table also gives the predicted moment capacities of the test beams using ε_{fd} calculated according to Eq. (3) and the comparison with the experimental results. The result of comparison indicates that the *fib* approach overly underestimates the debonding strain and the moment capacity of the test beams. The average ratio of $\varepsilon_{fd\ exp}/\varepsilon_{fd\ fib}$ was 2.54 with a coefficient of variation of 7% and the average ratio of the experimental to calculated capacities was 2.02 with a coefficient of variation of 6%.

4.3 JSCE design recommendations

The design recommendations of the Japan Society for Civil Engineers (JSCE) (1997) provide design equation for predicting the debonding strain of FRP laminates as follows:

$$\varepsilon_{fd} = \sqrt{\frac{2G_f}{nE_f t_f}} \tag{6}$$

where G_f is the interfacial fracture energy between FRP and concrete and its value can be taken as 0.5 N/mm.

Table 3 shows the comparison between the predicted debonding strain of the test beams using Eq. (6) and the experimental results. The table also gives the predicted moment capacities of the test beams considering ε_{fd} calculated according to Eq. (6) and the comparison with the experimental results. It can be seen that the JSCE method excessively underestimates both the debonding strain and the moment capacity of the test beams. The average ratio of $\varepsilon_{fd\ exp}/\varepsilon_{fd\ JSCE}$ was 2.98 with a coefficient of variation of 7%. Likewise, the average ratio of the experimental to calculated capacities was 2.35 with a coefficient of variation of 4%.

5 CONCLUSIONS

The test results of structurally damaged wide shallow reinforced concrete beams strengthened for flexure with externally-bonded CFRP plates were presented. The structural damaging was achieved by pre-cracking the beams under different loading levels. The effect of pre-damage on the efficiency of CFRP strengthening was investigated for two different reinforcement ratios of the external reinforcement. The CFRP reinforcement ratio was adjusted by maintaining the same thickness and changing the width of the plates. The test results were analyzed using the design guidelines of ACI 440.2R-08 (2008), the design recommendations of *fib* Bulletin 14 (2001), and the JSCE design recommendations (1997). The main findings of this study can be summarized as follows:

- All strengthened beams showed improved flexural performance in terms of ultimate capacity, flexural stiffness, and crack width control in comparison to the beam without external CFRP reinforcement.
- The strengthening efficiency and structural performance of pre-damaged beams, which had been preloaded to 35-95% of their unstrengthened ultimate strength and then plated, were found to be marginally influenced when compared with those of strengthened undamaged beams. A severely damaged beam, which had been preloaded to 95% of its ultimate strength, showed a reduction in the ultimate strength of 8% less than that of its counterpart strengthened undamaged beam. Thus, CFRP strengthening of damaged beams appears to be structurally efficient and reliable similar to strengthening of undamaged beams.
- A fully damaged RC beam can be properly repaired and strengthened giving comparable structural behavior to a strengthened beam that was not damaged before it was strengthened.
- The ACI 440.2R-08 design guide (2008) gave reasonable conservative predictions for the CFRP debonding strains and the ultimate capacities of the test beams including the preloaded strength-

ened beams. On the other hand, both *fib* Bulletin 14 (2001) and JSCE design recommendations (1997) led to unduly conservative predictions for the deboning strains and the ultimate capacities for all test beams.

Acknowledgement

The authors would like to acknowledge the financial support from the Center of Excellence for Research in Engineering Materials (CEREM) and the Center of Excellence for Concrete Research & Testing (CoE-CRT) at the College of Engineering - King Saud University. The help of the engineers and technicians in the CoE-CRT and in the structural laboratory of Civil Engineering Department at King Saud University is appreciated.

Nomenclature

The following symbols are used in this paper:

A_f = cross-sectional area of FRP reinforcement;
A_s = cross-sectional area of tension steel reinforcement;
A_s' = cross-sectional area of compression steel reinforcement;
b = width of beam;
b_f = width of FRP;
c = cracked transformed section neutral axis depth;
c_1 = factor equal to 0.64;
c_2 = factor equal to 2.0;
d = effective depth of tension steel;
d' = depth of compression steel;
E_f = modulus of elasticity of FRP reinforcement;
f_c' = specified compressive strength of concrete;
f_{ct} = tensile strength of concerte;
f_s = stress in tension steel;
f_s' = stress in compression steel;
h = total depth of beam;
k_c = factor accounting for the state of compaction of concrete;
k_b = geometry factor;
$l_{b,\,max}$ = maximum FRP bond length;
M_y = yield moment;
$M_{y\,cont}$ = yield moment of control beam;
M_u = ultimate moment;
$M_{u\,ACI}$ = ultimate moment calculated according to ACI 440;
$M_{u\,exp}$ = experimental ultimate moment;

$M_{u\,fib}$ = ultimate moment calculated according to *fib Bulletin 14*;

$M_{u\,JSCE}$ = ultimate moment calculated according to JSCE;

N = number of FRP plies;

t_f = thickness of FRP reinforcement;

w_y = crack width at yielding of tension steel;

w_u = crack width at ultimate moment;

α = reduction factor accounting for the influence of inclined cracks on the bond strength;

β_1 = ratio of depth of equivalent rectangular stress block to depth of the neutral axis;

δ_y = deflection at yielding of tension steel;

δ_u = deflection at ultimate moment;

ε_{fd} = FRP debonding strain;

$\varepsilon_{fd\,ACI}$ = FRP debonding strain calculated according to ACI 440;

$\varepsilon_{fd\,exp}$ = experimental FRP debonding strain;

$\varepsilon_{fd\,fib}$ = FRP debonding strain calculated according to *fib Bulletin 14*;

$\varepsilon_{fd\,JSCE}$ = FRP debonding strain calculated according to JSCE;

ε_{fu} = design rupture strain of FRP reinforcement;

ρ_f = reinforcement ratio of FRP;

ψ_f = reduction factor;

References

ACI 440.2R-08. (2008). Guide for the design and construction of externally bonded FRP systems for strengthening concrete structures. American Concrete Institute.

Al-Negheimish, A. I., El-Sayed, A. K., Al-Zaid, R. A., Shuraim, A. B., Alhozaimy, A. M. (2012). Behavior of wide shallow RC beams strengthened with CFRP reinforcement, Journal of Composites for Construction, ASCE, 16(4): 418-429.

Al-Zaid, R. A., Al-Negheimish, A. I., Al-Saawani, M. A., El-Sayed, A. K. (2012). Analytical study on RC beams strengthened for flexure with externally bonded FRP reinforcement. Composites Part B: Engineering, 43(2): 129-141.

Aram, M. R., Czaderski, C., Motavalli, M. (2008). Debonding failure modes of flexural FRP-strengthened RC beams, Composites Part B: engineering, 39: 826-841.

Arduini, M., Nanni, A. (1997). Behavior of precracked RC beams strengthened with carbon FRP sheets, Journal of Composites for Construction, ASCE, 1(2): 63-70.

Bencardino, F., Spadea, G., Swamy, R. N. (2002). Strength and ductility of reinforced concrete beams externally reinforced with carbon fiber fabric, ACI Structural Journal, 99(3): 163-171.

Fédération Internationale du Béton. (2001). Externally bonded FRP reinforcement for RC structures. fib Bulletin 14.

Jayaprakash, J., Pournasiri, E., Choong, K. K., Tan, C. G., De'nan, F. (2011). External CFRP repairing of pre-tested beams reinforced using prestress rebars, Journal of Reinforced Plastics and Composites, 30(20): 1753-1768.

JSCE. (1997). Recommendations for upgrading of concrete structures with use of continuous fiber sheets. Japan Society for Civil Engineers, Japan.

Liu, I. S. T., Oehlers, D. J., Seracino, R., (2007). Study of intermediate crack debonding in adhesively plated beams, Journal of Composites for Construction, ASCE, 11(2):175-183.

Rabinovitch, O., Frostig, Y., (2003). Experimental and analytical comparison of RC beams strengthened with CFRP composites, Composites Part B: engineering, 34: 663-673.

Rahimi, H., Hutchinson, A. (2001). Concrete beams strengthened with externally bonded FRP plates, Journal of Composites for Construction, ASCE, 5(1): 44-56.

Rosenboom, O., Rizkalla, S. (2008). Experimental study of intermediate crack debonding in fiber-reinforced polymer strengthened beams, ACI Structural Journal, 105 (1): 41-50.

Shahawy, M., Chaallal, O., Beitelman, T., El-Saad, A. (2001). Flexural strengthening with carbon fiber-reinforced polymer composites for preloaded full-scale girders, ACI Structural Journal, 98 (5): 735-742.

Shin, Y. S., Lee, C. (2003). Flexural behavior of reinforced concrete beams strengthened with carbon fiber-reinforced polymer laminates at different levels of sustaining load, ACI Structural Journal, 100(2): 231-239.

Shuraim, A. B., Al-Negheimish, A. I. (2011). Design considerations for joist floors with wide-shallow beams, ACI Structural Journal, 108(2):188–196.

Sika carboDur plates. (2009). Product data sheet, Sika services, Switzerland, 7p.

Sikadur-30. (2009). Product data sheet, Sika services, Switzerland, 6p.

Teng, J. G., Smith, S. T., Chen, J. F. (2003). Intermediate crack-induced debonding in RC beams and slabs, Construction and Building Materials, 17: 447-462.

The Concrete Society. (2004). Design guidance for strengthening concrete structures using fibre composite materials. Technical report 55, UK, 128 pp.

Yao, J., Teng, J. G., Lam, L. (2004). Experimental study on intermediate crack debonding in FRP-strengthened RC flexural members, Advances in Structural Engineering, 8(4):365-395.